Efficiency of random search with space-dependent diffusivity

M. A. F. dos Santos [1], L. Menon, Jr.,[1] and C. Anteneodo [1,2]

[1]*Department of Physics, PUC-Rio, Rua Marquês de São Vicente 225, 22451-900 Rio de Janeiro, Brazil*
[2]*Institute of Science and Technology for Complex Systems, INCT-SC, Brazil*

We address the problem of random search for a target in an environment with a space-dependent diffusion coefficient $D(x)$. Considering a general form of the diffusion differential operator that includes Itô, Stratonovich, and Hänggi-Klimontovich interpretations of the associated stochastic process, we obtain and analyze the first-passage-time distribution and use it to compute the search efficiency $\mathcal{E} = \langle 1/t \rangle$. For the paradigmatic power-law diffusion coefficient $D(x) = D_0 |x|^{\alpha}$, where x is the distance from the target and $\alpha < 2$, we show the impact of the different interpretations. For the Stratonovich framework, we obtain a closed-form expression for $\mathcal{E}$, valid for arbitrary diffusion coefficient $D(x)$. This result depends only on the distribution of diffusivity values and not on its spatial organization. Furthermore, the analytical expression predicts that a heterogeneous diffusivity profile leads to a lower efficiency than the homogeneous one with the same average level within the space between the target and the searcher initial position, but this efficiency can be exceeded for other interpretations.

I. INTRODUCTION

Finding efficient strategies that minimize the time to encounter a target, or optimize other search criteria, is crucial in diverse contexts and at different scales [1–3]. At the molecular level, let us mention the search of a protein for its binding site on DNA [4–6], and at the ecological scales, the search for food (foraging) or viable habitats [7–11]. Other applications include design in robotics [12] or computer algorithms to find minima in a complex landscape [13].

Among the fundamental studies on random searches, several diffusion processes have been investigated, for instance, Lévy flights [13,14], fractional Brownian motion [15], run-and-tumble motion [16], and diffusion with resetting [17,18]. However, in many complex environments, the diffusivity cannot be considered uniform, but changes from one point to another [19,20], and this may have important consequences in random searches. State-dependent diffusivity has been considered in the context of infinite-ergodic theory [21], biologically motivated problems [22–25], stock markets [26], and many others.

In one dimension, a single trajectory $x(t)$ can be modeled by the following stochastic process:

$$\dot{x} = \sqrt{2D(x^*)}\,\eta(t), \tag{1}$$

where x is the spatial coordinate (or other state variable, such as chemical coordinate or stock prize), $D(x) > 0$ is the diffusion coefficient, and $\eta(t)$ is a zero-mean white noise with delta correlation $\langle \eta(t + t')\eta(t) \rangle = \delta(t')$. However, due to the multiplicative white noise, the integration of Eq. (1) requires specifying the instant at which $D(x^*)$ is computed [27], and we consider $x^* = [(2 - A)\,x(t + dt) + A\,x(t)]/2$ [28], where $0 \leqslant A \leqslant 2$. The case $A = 2$ (Itô), commonly used in finance, has a nonanticipating property [29], while $A = 1$ (Stratonovich) is an anticipating choice, which

obeys the rules of usual calculus [30]. The highly anticipating case $A = 0$ (known as isothermal, kinetic, or Hänggi-Klimontovich) [20,31,32] has applications related to Fick's law [33,34]. Other values of A have also been considered in previous literature [35]. In any case, the stochastic Eq. (1) can be cast, for instance, in the form

$$\dot{x} = (1 - A/2)D'(x) + \sqrt{2D(x)}\,\eta(t), \tag{2}$$

which corresponds to the Itô scheme, suitable for numerical integration, with noise amplitude ruled by $x(t)$, but with an additional drift term which vanishes in the Itô case ($A = 2$), as well as for homogeneous diffusivity, because $D'(x) = dD/dx = 0$. The corresponding heterogeneous diffusion equation is

$$\partial_t p(x, t) = \partial_x \{D(x)^{1-A/2}\partial_x[D(x)^{A/2}p(x, t)]\}, \tag{3}$$

where $p(x, t)$ is the probability density function (PDF). The anticipating character, reflected in the value of A, has an impact on the spreading of particles and on the tails of $p(x, t)$, as well as produces diffusion anomalies and ergodicity breaking [19,21,36,37], and hence is expected to affect search processes.

Fundamental aspects related to stochastic search in heterogeneous diffusivity media have been studied for particular forms of the diffusivity, for instance, in a confined setting within Hänggi-Klimontovich interpretation (theoretically) [38], within Stratonovich scheme (numerically) [39], in layered media for arbitrary interpretation [28], or with stochastic resetting [40,41]. The step shape of the diffusivity profile in a confined and d-dimensional system was investigated in Ref. [28] for all interpretations. In all these cases, the mean first-passage time (MFPT) was calculated, but the average of the inverse time (efficiency) is another relevant quantity, for instance for random search on a comb

model [42], and especially when the mean passage time is divergent.

Our purpose is to characterize the performance of one-dimensional random searches in nonconfined heterogeneous media with different forms of $D(x)$ and interpretations of the heterogeneous diffusion process (HDP). In particular, within Stratonovich interpretation, we will be able to find general results for arbitrary $D(x)$.

A target can be introduced into the diffusion equation (3) by means of a δ-delta sink term or by means of absorbing boundary conditions. We will use the latter approach. Moreover, we consider that a searcher follows a HDP, exploring all points along its trajectory [2]. To study random searches, it is central to determine the first-passage-time distribution (FPTD),

$$\wp(t) = -\frac{d}{dt}Q(x_0, t), \quad (4)$$

where x_0 is the initial position of the walker, $Q(x_0, t) = \int_\Omega p(x, t|x_0)dx$, with support Ω the survival probability at time t. The FPTD represents the probability density of the first time the walker meets the target, after which the walker is removed from the system [1,27]. Therefore, note that the norm of the density $p(x, t|x_0)$ is not conserved.

To quantify and compare the performance of different search processes, a fundamental measure is the so-called search efficiency, and various definitions can be found in Ref. [43]. We will use a definition close to the step efficiency (inverse of the traveled time up to reaching the target) [44], namely,

$$\mathcal{E} = \langle t^{-1} \rangle = \int_0^\infty t^{-1}\wp(t)dt = \int_0^\infty \widetilde{\wp}(s)ds, \quad (5)$$

where $\widetilde{\wp}(s)$ is the Laplace transform of the FPTD. The measure defined by Eq. (5) is adequate for systems where the mean arrival time diverges [44]. $\mathcal{E}$ is the first-order negative moment, which preferentially weights the contribution of short arrival times, dismissing trajectories that take very long times to reach the target. It has been used in a series of works to characterize the performance of Lévy searches, facing multiples targets [14], under external bias [45], comb structures [46], asymmetric Lévy flights [47], and to describe long relocations mingled with thorough local exploration [48].

Our results are organized as follows. In Sec. II, we start from the backward Fokker-Planck equation, with arbitrary A, to obtain the first-passage-time distribution and, using it, the search efficiency when the position-dependent diffusivity has a power-law form, which has been used in different frameworks [19,41,49]. In Sec. III, we obtain a closed expression for the efficiency, valid for arbitrary $D(x)$ within the Stratonovich scheme ($A = 1$). In all cases, examples and comparisons of the theory with stochastic simulations are provided. Final remarks are presented in Sec. IV.

II. RANDOM SEARCH IN MEDIA WITH POWER-LAW DIFFUSIVITY UNDER DIFFERENT PRESCRIPTIONS

A. Survival probability

We consider independent random walkers on a one-dimensional heterogeneous medium, initially located at posi-

tion x_0, i.e., the initial density function is $p(x, 0) = \delta(x - x_0)$ and its evolution is described by Eq. (3), which for differentiable $D(x)$ can be rewritten as

$$\frac{\partial}{\partial t}p(x, t|x_0) = \frac{\partial^2}{\partial x^2}\{D(x)p(x, t|x_0)\}$$

$$+ (A/2 - 1)\frac{\partial}{\partial x}\left\{\frac{dD(x)}{dx}p(x, t|x_0)\right\}. \quad (6)$$

In this format, the diffusion term is of the Itô form but a spurious drift term appears, which vanishes for $A = 2$. This representation will be useful to obtain the survival probability.

To address the random search problem, we consider, without loss of generality, that a target is located at $x = 0$, which corresponds to a change of coordinate. The target position defines a bound of the search domain because we are considering a cruise search in which the walker can detect the target during its movement, and it is removed when the target is first detected. Without loss of generality, we assume that the initial position of the random searcher is $x_0 > 0$, in which case the search domain is the positive x axis $[0, \infty)$.

Regarding the heterogeneous diffusivity, in this section we will focus our analyses on the power-law case,

$$D(x) = D_0 x^\alpha, \quad (7)$$

where $x \geqslant 0$ and $\alpha < 2$. This kind of profile has been used to capture the diffusive motion of a particle on fractal objects [50] and diffusion in turbulent media [42]. It has also been used as a paradigm of heterogeneous diffusivity to study infinite ergodic theory [21], extreme value statistics [51], and critical habitat size of biological populations [24]. In the current problem, we can interpret that the target modifies the diffusivity around it, making it increase ($\alpha > 0$) or decrease ($\alpha < 0$) with the distance from the target at the origin. Then, it may be a good candidate profile to model animal search in which the target emits cues (e.g., odors [52–54] or sounds [10,55]).

In Fig. 1, we show typical trajectories, obtained by integrating Eq. (2), when the diffusivity has the power-law form $D(x) = D_0 x^\alpha$, with $\alpha = \pm 0.5$ and an absorbing boundary at $x = 0$, for three different values of A. For each interpretation, the stochastic term is the same (and we used the same random sequence of the noise for comparison), but the deterministic drift term is enhanced when the process is more anticipating (smaller A). Moreover, the drift term is either positive (if $\alpha > 0$) or negative (if $\alpha < 0$); then a more anticipating rule will make the walker reach the origin for the first time earlier or later, respectively, as observed in each panel of Fig. 1.

The survival probability $Q(x_0, t) = \int_0^\infty p(x, t|x_0)dx$ represents the probability that the diffusing particle, starting at x_0, has not hit the target ($x = 0$) up to time t. It can be determined through the backward Fokker-Planck equation [27], which, for the chosen power law $D(x)$, reads

$$\frac{\partial}{\partial t}Q(x_0, t) = D_0 x_0^\alpha \frac{\partial^2}{\partial x_0^2}Q(x_0, t)$$

$$+ \frac{(1 - A/2)D_0\alpha}{x_0^{1-\alpha}}\frac{\partial}{\partial x_0}Q(x_0, t), \quad (8)$$
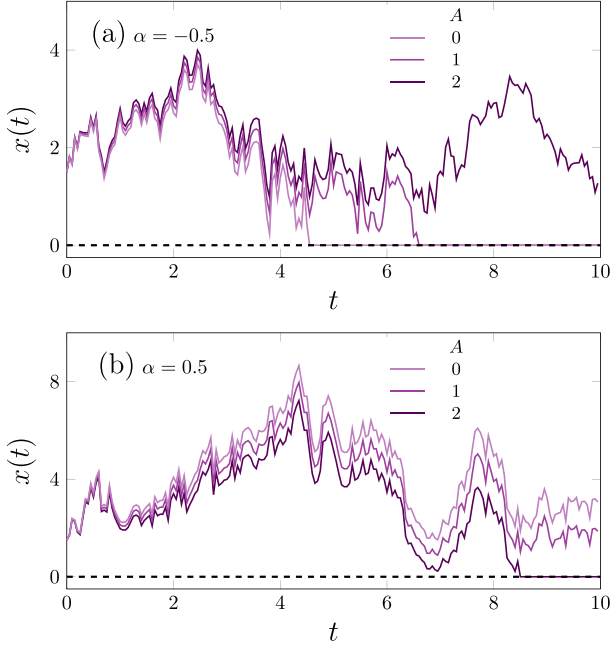
FIG. 1. Random trajectories with $D(x) = D_0 x^\alpha$ and an absorbing boundary at $x = 0$ (dashed line), for (a) $\alpha = -0.5$ and (b) $\alpha = 0.5$. We set $D_0 = 1.0$, $x_0 = 1.5$, and the integration of Eq. (2) was performed using the stochastic Euler algorithm with adaptive time step. In each panel, the same random sequence was used, for comparison.

together with the boundary condition $Q(0, t) = 0$, meaning that the survival probability is null when the walker starts at the target position $x_0 = 0$. The initial condition is $Q(x_0 > 0, 0) = 1$ since $p(x, 0|x_0) = \delta(x - x_0)$ and $x_0 \in (0, \infty)$.

The Laplace transform, defined as $\tilde{f}(s) = \int_0^\infty f(t) e^{-st} dt$, applied on the time variable of Eq. (8), implies

$$s\tilde{Q}(x_0, s) - 1 = D_0 x_0^\alpha \frac{\partial^2}{\partial x_0^2} \tilde{Q}(x_0, s)$$
$$+ \frac{(1 - A/2)D_0\alpha}{x_0^{1-\alpha}} \frac{\partial}{\partial x_0} \tilde{Q}(x_0, s), \quad (9)$$

which can be solved analytically, as shown in Appendix A, obtaining

$$\tilde{Q}(x_0, s) = \frac{1}{s} - \frac{2}{\Gamma[b] s} \left(\frac{x_0^{\frac{2-\alpha}{2}}}{2 - \alpha} \sqrt{\frac{s}{D_0}} \right)^b$$
$$\times K_b \left(\frac{2 x_0^{\frac{2-\alpha}{2}}}{2 - \alpha} \sqrt{\frac{s}{D_0}} \right), \quad (10)$$

where $K_b(z)$ is the modified Bessel function and

$$b = \frac{1 - \alpha(1 - A/2)}{2 - \alpha}, \quad (11)$$

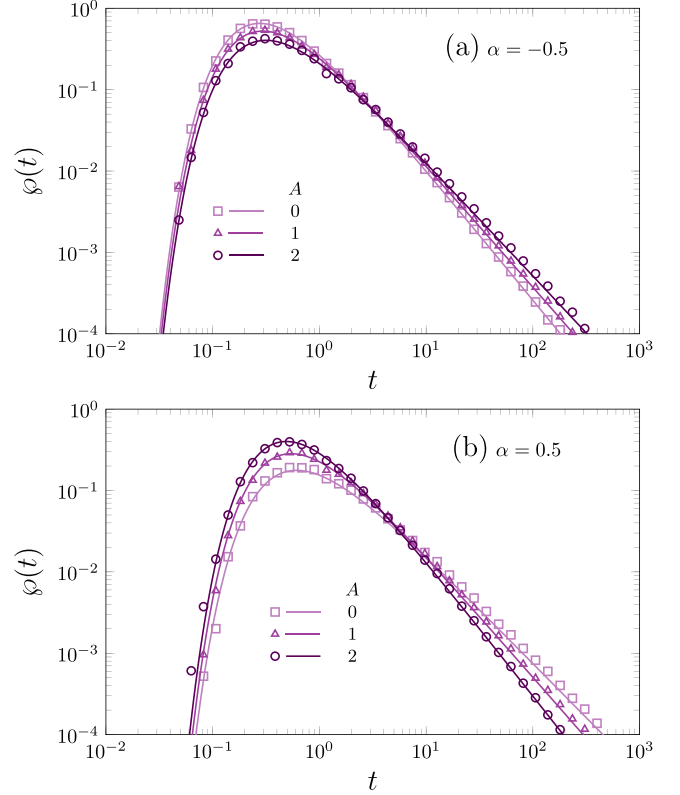with the restriction $1 - \alpha(1 - A/2) \geqslant 0$. See Eq. (A11) in Appendix A.

FIG. 2. First-passage-time distribution (FPTD) given by Eq. (13) (solid lines) and from 10^5 trajectories obtained from Eq. (2) with absorbing boundary at $x = 0$ (symbols), for the HDP with $D(x) = D_0 x^\alpha$. (a) $\alpha = -0.5$, (b) $\alpha = 0.5$. In all cases, $x_0 = 1.0$ and $D_0 = 1.0$. In simulations, for $t < 1$ we used $dt = 10^{-4}$, and for $t \geqslant 1$ we used $dt = 10^{-2}$.

B. First-passage-time distribution

From Eq. (4), the Laplace transform of the FPTD is given by $\tilde{\wp}(s) = 1 - s\tilde{Q}(x_0, s)$; then,

$$\tilde{\wp}(s) = \left(\frac{x_0^{\frac{2-\alpha}{2}}}{2 - \alpha} \sqrt{\frac{s}{D_0}} \right)^b \frac{2}{\Gamma[b]} K_b \left(\frac{2 x_0^{\frac{2-\alpha}{2}}}{2 - \alpha} \sqrt{\frac{s}{D_0}} \right). \quad (12)$$

To perform Laplace inversion, we use $\mathcal{L}^{-1}\{s^{\frac{b}{2}} K_b(d\sqrt{s})\} = \exp(-d^2/[4t]) d^b/(2t)^{b+1}$ [56], which implies

$$\wp(t) = \frac{1}{\mathcal{Z}(2t)^{b+1}} e^{-\frac{x_0^{2-\alpha}}{(2 - \alpha)^2 D_0 t}}, \quad (13)$$

with

$$\mathcal{Z}^{-1} = 2 \left(\frac{2}{2 - \alpha} \right)^{2b} \frac{x_0^{1-\alpha(1-A/2)}}{(2D_0)^b \Gamma(b)}, \quad (14)$$

recalling that from Eq. (11), it must be $\alpha(1 - A/2) < 1$ for the FPTD to be normalizable. In the particular case where $A = 2$ (Itô interpretation) and $\alpha = 1$, Eq. (13) gives $\wp(t) = (x_0/D_0)t^{-2} \exp[-x_0/(D_0 t)]$, recovering previous results [40].

Figure 2 shows the very good correspondence between the obtained FPTD from the analytical prediction given by Eq. (13) and from simulations of Eq. (2) with absorbing wall at $x = 0$, for different values of A. For instance, in the case

$\alpha = -0.5$ [Fig. 2(a)], notice that for a walker with larger A, the probability of short times diminishes and tails are longer, two features that contribute to the tendency shown in Fig. 1, delaying the encounter of the walker with the absorbing wall. The opposite occurs in the case $\alpha = 0.5$ [Fig. 2(b)], also in accord with Fig. 1.

Moreover, the asymptotic behavior of $\wp(t)$ in Eq. (13) indicates that normalization is possible when $\alpha < 2$ ($A = 1, 2$) or $\alpha < 1$ ($A = 0$), which also implies the existence of the efficiency $\mathcal{E}$. The mean first-passage time $\langle t \rangle$ is finite only for $A = 2$ and $1 < \alpha < 2$, which is the reason it would not be a good measure to characterize the performance of the considered processes.

C. Search efficiency

The search efficiency, defined in Eq. (5), can be calculated using Eq. (12), which gives

$$\mathcal{E} = \frac{D_0}{x_0^{2-\alpha}} \left(1 - \frac{2-A}{2} \alpha \right) (2 - \alpha). \quad (15)$$

This equation (15) summarizes the effects of the heterogeneity produced by α, under different interpretations. When $\alpha = 0$, the standard efficiency for the homogeneous case, $\mathcal{E}_H = 2D_0/x_0^2$ [14], is recovered. In Fig. 3, we show plots of $\mathcal{E}$ as a function of α, for different values of A, generated from Eq. (15), in agreement with the results of simulations of the stochastic Eq. (2). In Figs. 3(a) and 3(b), where $x_0 > 1$, we note that there is an optimal value $\alpha_{\max}$, which is shifted to the right the less anticipatory the process is (the larger A). The optimal efficiency $\mathcal{E}(\alpha_{\max})$, which decays with x_0 as expected, is enhanced for larger A for large enough x_0 [Fig. 3(a)], but this tendency is inverted in the case shown in Fig. 3(b). For $x_0 \leqslant 1$ [Fig. 3(c)], the efficiency monotonically decreases with α, for any A, diverging for $\alpha \to -\infty$.

As a general feature, we notice that for fixed x_0 and fixed α, the interpretation of HDP modifies the efficiency. When the diffusivity increases with the distance to the target ($\alpha > 0$), the efficiency is higher, the less anticipating the process is (i.e., the larger A is), but the efficiency is reduced otherwise. Then, a given behavior of the diffusivity around the target (ruled by α) can be influenced by the correlations (ruled by A) in the motion of the searcher. Processes characterized by different values of A will have different performance. Therefore, describing a given process with an inadequate value of A may lead to a wrong estimation of the efficiency.

III. RANDOM SEARCH WITHIN THE STRATONOVICH SCENARIO

In this section, we address the search problem within the Stratonovich framework, for which we will be able to obtain results for general $D(x)$. The Stratonovich HDP is the particular case of Eq. (3), setting $A = 1$, namely,

$$\frac{\partial}{\partial t} p(x, t|x_0) = \frac{\partial}{\partial x} \sqrt{D(x)} \frac{\partial}{\partial x} \sqrt{D(x)} p(x, t|x_0), \quad (16)$$

with $p(\pm\infty, t|x_0) = 0$ and $p(x, 0|x_0) = \delta(x - x_0)$. This equation corresponds to the stochastic process defined by Eq. (2) with $A = 1$. It is interesting to note that Eq. (16) also arises in
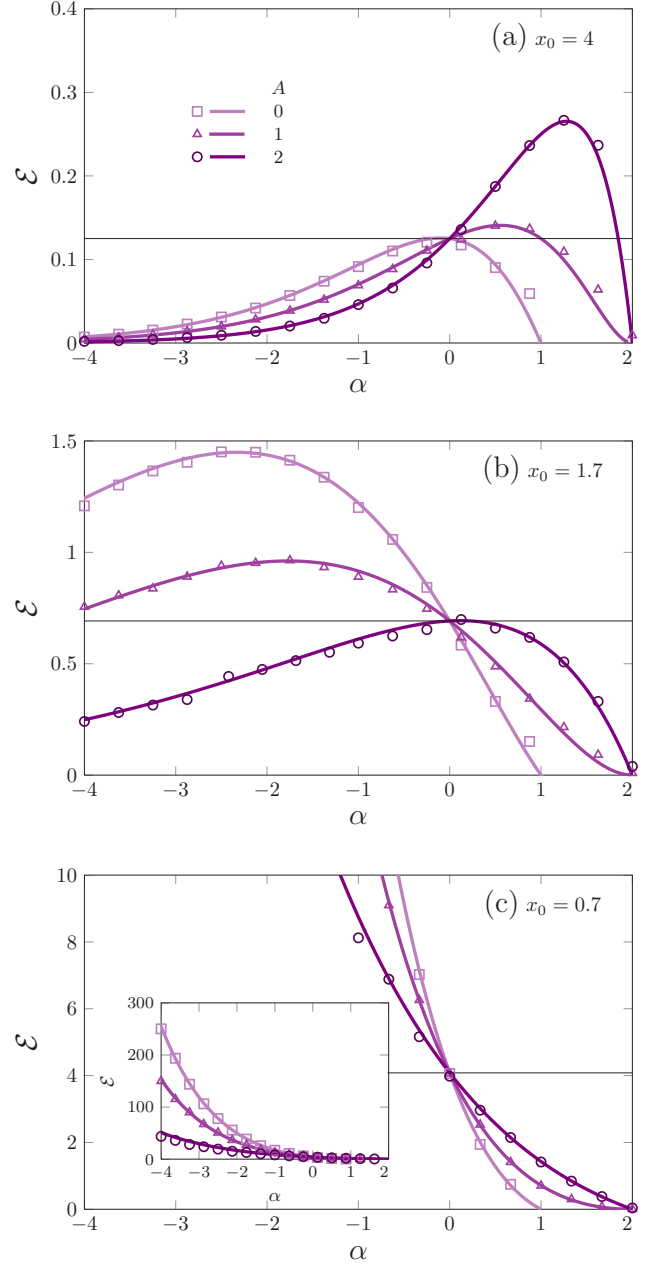

FIG. 3. Efficiency vs α for different interpretations of the HDP (values of A indicated in the legend), using $D(x) = D_0 x^\alpha$, with $D_0 = 1$. Each panel corresponds to a different value of x_0. The prediction given by Eq. (15) is shown by solid lines, and the average over 10^5 realizations of Eq. (2) with absorbing boundary at $x = 0$ is represented by symbols. In each case, the average over is shown. The solid horizontal line corresponds to the homogeneous value $\mathcal{E}_H = 2D_0/x_0^2$.

the context of run-and-tumble motion with space-dependent velocity [57].

To address the search problem, we first solve the diffusion equation (16) without a target and use the free solution to reproduce the boundary condition of the search problem through the method of images.
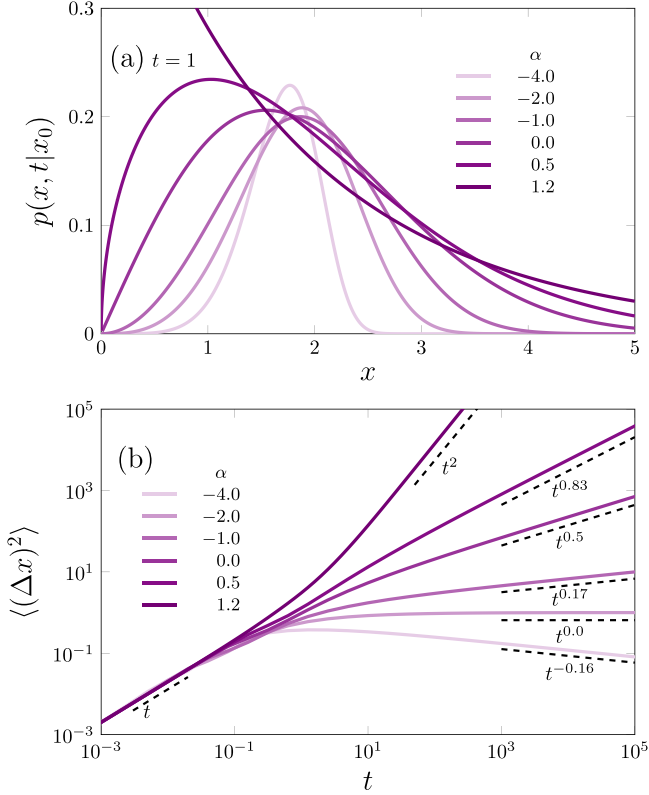
FIG. 4. (a) PDF vs x at $t = 1$ and (b) MSD vs t, for $D(x) = D_0 x^\alpha$, with D_0, and different values of α indicated in the legend. In (a), the area under the curves smaller than unit is due to the loss of norm. In (b), we can observe that for short times, diffusion is normal, but for long times, MSD $\sim t^{\frac{2+\alpha}{2(2-\alpha)}}$.

Using the change of variables [24],

$$y(x) = \int_0^x \frac{1}{\sqrt{D(x')}} dx', \tag{17}$$

which allows one to rewrite Eq. (16) as $\partial_t \tilde{P}(y, t) = \partial_{yy}^2 \tilde{P}(y, t)$, where $\tilde{P}(y(x), t) = \sqrt{D(x)}\, p(x, t)$. Its natural solution, for $y \in (-\infty, \infty)$, is $\tilde{P}_0(y, t) = \exp[-y^2/(4t)]/\sqrt{4\pi t}$. To reproduce an absorbing wall at the origin, i.e., $\tilde{P}[y(x = 0), t] = 0$, we apply the method of images to the free solution with initial condition $\tilde{P}[y(x), 0] = \delta(y - y_0)$, which implies $\tilde{P}(y, t) = \tilde{P}_0(y - y_0, t) - \tilde{P}_0(y + y_0, t)$. After that, we obtain

$$p(x, t|x_0) = \frac{\tilde{P}(y, t)}{\sqrt{D(x)}} = \sum_{k=-1,1} k \frac{e^{-\frac{[y(x) - k\, y(x_0)]^2}{4t}}}{\sqrt{4\pi D(x)t}}. \tag{18}$$

This expression works for any space-dependent diffusivity [allowing the change $y(x)$].

An illustrative example of the PDF at a given time ($t = 1$) is presented in Fig. 4 for the power-law diffusion coefficient given by Eq. (7), with different values of α. Notice the loss of norm, visibly more pronounced with decreasing α, which favors adsorption. Besides the PDF, we show the mean square displacement (MSD) versus time. At early times, the MSD increases linearly with time for any α, meaning a normal diffusion spread. However, for long times, we observe an unusual behavior of the MSD, namely, $\langle (\Delta x)^2 \rangle \propto t^{\frac{2+\alpha}{2(2-\alpha)}}$. See

the derivation in Appendix B. When $\alpha = -2$, the MSD becomes stationary but the PDF keeps losing norm. For $\alpha < -2$, besides losing norm, the PDF narrows with time as reflected by the negative exponent in the MSD.

The integration of Eq. (18) over x yields the survival probability

$$Q(x_0|t) = \int_0^\infty \frac{e^{-\frac{[y - y(x_0)]^2}{4t}} - e^{-\frac{[y + y(x_0)]^2}{4t}}}{\sqrt{4\pi t}} dy = \mathrm{erf}\left(\frac{y(x_0)}{2t^{\frac{1}{2}}} \right), \tag{19}$$

where erf is the error function.

The FPTD can be obtained directly from Eq. (19) using Eq. (4), namely,

$$\wp(t) = \frac{y(x_0) e^{-\frac{y(x_0)^2}{4t}}}{2\sqrt{\pi} t^{\frac{3}{2}}}. \tag{20}$$

When $D(x)$ is a power law, we recover the result of Eq. (13) for $A = 1$.

Using $\wp(t)$ in Eq. (20), we compute the efficiency defined in Eq. (5), $\mathcal{E} = \langle t^{-1} \rangle = \int \wp(t) t^{-1} dt$, and through the change of variables $\xi = y_0^2/(4t)$, we have $\mathcal{E} = \frac{4}{y_0^2} \int_0^\infty \frac{e^{-\xi}}{\sqrt{\pi}} \xi^{\frac{1}{2}} d\xi = \frac{2}{y_0^2}$. Therefore,

$$\mathcal{E} = \frac{2}{\left| \int_0^{x_0} [D(x')]^{-\frac{1}{2}} dx' \right|^2}, \tag{21}$$

valid for arbitrary diffusivity profile $D(x)$. Notice that the efficiency only depends on the profile within the interval $(0, x_0)$. Moreover, notice that since the integrand is a function of $D(x)$ only, the efficiency does not depend on the particular sequence of values of the diffusivity. That is, if we fragment the profile and shuffle the fragments [24], the value of the integral will be the same.

Moreover, to put into evidence the variations ξ around a reference level D_0, we write $D(x) = D_0[1 + \xi(x)]$, such that $\langle \xi \rangle = 0$ for $x \in [0, x_0]$, and $\xi > -1$ for the positivity of D. Under such constraints for $\{\xi_i\}$, it is easy to show that $\sum_{i=1}^N [1 + x_i]^{-1/2}/N \geqslant 1$ [24]; then, in the continuous limit, $y_0 \geqslant x_0/\sqrt{D_0}$, which implies

$$\mathcal{E} = \frac{2}{y_0^2} \leqslant \frac{2D_0}{x_0^2} = \mathcal{E}_H. \tag{22}$$

This means that the efficiency of a heterogeneous profile is lower than that of a homogeneous profile with a level equal to the average of the heterogeneous one.

Below we provide two concrete examples: a localized break of homogeneity and an oscillatory profile. In addition, we will discuss the case of a stochastic profile.

A. Localized heterogeneity

We analyze a profile that presents a local perturbation of the diffusivity around the level D_0. The average diffusivity is conserved, as far as the perturbation is contained within the interval $[0, x_0]$. The local heterogeneity depicted in Fig. 5 has width $0 \leqslant w \leqslant x_0$ and amplitude $0 \leqslant h \leqslant 1$. For this layered
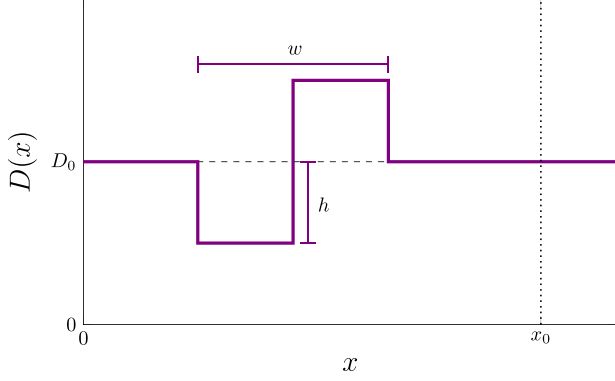
FIG. 5. Localized heterogeneity of width w and amplitude h, around the level D_0 in dashed line. The dotted vertical line highlights the initial position.

diffusivity, Eq. (21) straightforwardly yields

$$\mathcal{E} = \frac{2D_0}{\left(x_0 - w + w\frac{\sqrt{1+h}+\sqrt{1-h}}{2\sqrt{1-h^2}}\right)^2} \leqslant \mathcal{E}_H. \qquad (23)$$

For $w = 0$ or $h = 0$, the standard value $\mathcal{E}_H$ is recovered, while for increasing w and $|h|$, the efficiency decays, as can be visualized in Fig. 6. This means that in a heterogeneous profile that preserves the average, within the Stratonovich framework, the search is less efficient than in a homogeneous environment with the average diffusivity. Let us also note that according to Eq. (21), a rigid shift of the pulse will not affect the efficiency, as soon as the pulse remains contained within the integration interval $[0, x_0]$. Also, fragmentation of the pulse into smaller ones will produce the same $\mathcal{E}$, as far as the total length of up and down diffusivities is the same. Moreover, notice that although Eq. (3) is the same for any A in each region where the diffusivity is constant, as well as the continuity condition for the density flux at the interface $D_1\partial_x p_1 = D_2\partial_x p_2$, the condition for the density $D_1^{A/2}p_1 = D_2^{A/2}p_2$ depends on A [28]. Therefore, $\mathcal{E}$ may depend on the value of A.
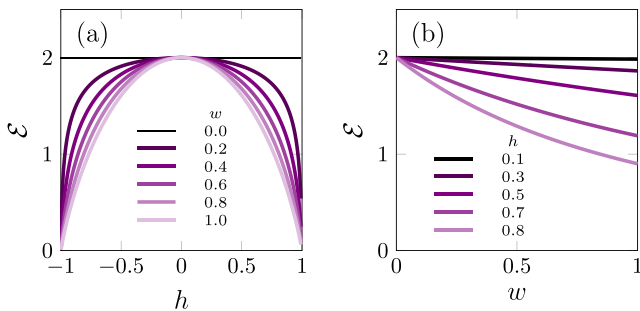

FIG. 6. Efficiency for the landscape sketched in Fig. 5, varying h and w. Notice that in all cases, the efficiency is lower than that for the homogeneous case. The horizontal lines correspond to $\mathcal{E}_H$ which is the value for the homogeneous case with the same average.
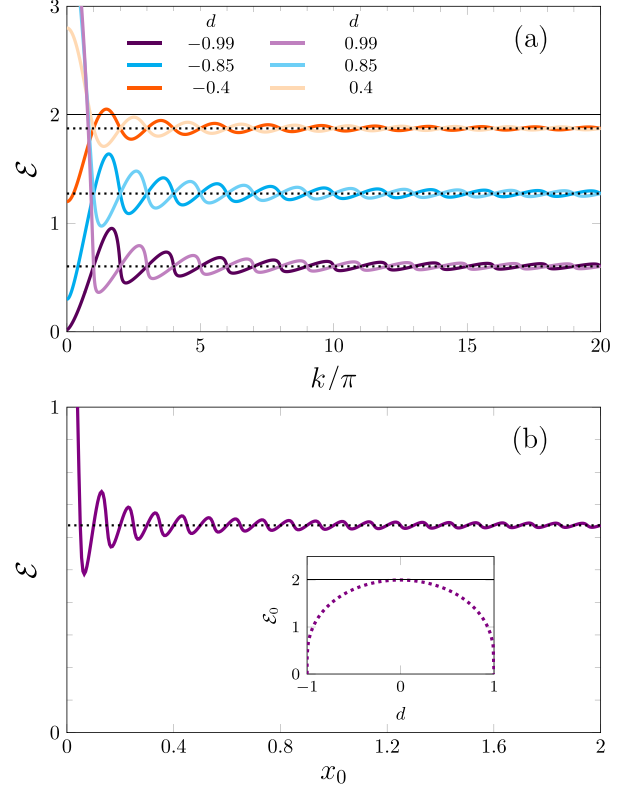

FIG. 7. (a) Efficiency $\mathcal{E}$ for $D(x) = D_0[1 + d\cos(kx)]$ vs k, for different values of d. The dotted horizontal lines correspond to the respective short-wavelength limit given by Eq. (25). We set $x_0 = 1$ and $D_0 = 1$. (b) $\mathcal{E}$ vs x_0, for $k = 20\pi$, $D_0 = 1$, and $d = 0.85$. Inset: The short-wavelength limit $\mathcal{E}_0$ (dashed line) vs d and, for comparison, the efficiency of the corresponding homogeneous case $\mathcal{E}_H$ (thin horizontal line).

B. Oscillating diffusivity

As a paradigm of an oscillatory landscape, we analyze the sinusoidal diffusivity kernel

$$D(x) = D_0 [1 + d\cos(kx)], \qquad (24)$$

where oscillations occur around the reference level D_0, with $-1 \leqslant d \leqslant 1$ and wave number k. We integrated numerically the general expression for the efficiency, given by Eq. (21), using $D(x)$ in Eq. (24), and show the results in Fig. 7.

For a fair comparison with the homogeneous case, let us consider oscillations whose average around D_0 vanishes. This occurs when $kx_0 = N\pi$, with integer N, and also in the limit of very short wavelength compared to x_0 (i.e., $\lambda = 2\pi/k \ll x_0$). For integer N, we obtain

$$\mathcal{E}_0 \simeq \mathcal{E}_H \frac{(1+d)\pi^2}{4\left[\kappa\left(\frac{2d}{1+d}\right)\right]^2} \leqslant \mathcal{E}_H, \qquad (25)$$

where $\kappa(z) = \frac{\pi}{2}\,_2F_1(\frac{1}{2}, \frac{1}{2}, 1, z)$ is the complete elliptic integral of the first kind. The short-wavelength limit $\mathcal{E}_0$, for each d, is plotted in Fig. 7 by dotted horizontal lines. Notice that, in fact, it is attained for integer N or large k. This limit value is independent of the introduction of a phase constant in Eq. (24), as can be observed when d changes sign. More

importantly, Eq. (25) is maximal at $d = 0$ where it takes the value $\mathcal{E}_H$. That is, the efficiency $\mathcal{E}_0$ remains below that of the homogeneous case with the same average diffusivity. This is a noticeable result that indicates that short-wavelength oscillations of the diffusivity spoil the efficiency of the search, which decays with increasing d, as represented by the dashed line in Fig. 7(b). In contrast, for small values of k, the value of the efficiency can be higher than $\mathcal{E}_H$, but this simply reflects an average diffusivity higher than D_0 within the interval $[0, x_0]$.

C. Random diffusivity

As discussed in connection with Eq. (22), shuffled diffusivity profiles in the interval $(0, x_0)$ yield the same efficiency within the Stratonovich framework. This leads one to consider noisy diffusivity profiles $D(x) = D_0(1 + \xi)$, around the level D_0, taking uncorrelated random values ξ with a given PDF $f(\xi)$, where $\xi \in (-1, \infty)$, such that the average $\langle \xi \rangle = \int_{-1}^{\infty} \xi f(\xi) d\xi = 0$. Following this idea, Eq. (21) can be rewritten as

$$\mathcal{E} = \frac{\mathcal{E}_H}{\left(\int_{-1}^{\infty} [1 + \xi]^{-\frac{1}{2}} f(\xi) d\xi \right)^2} \leqslant \mathcal{E}_H, \qquad (26)$$

where the upper bound comes from the inequality [24]

$$\int_{-1}^{\infty} [1 + \xi]^{-\frac{1}{2}} f(\xi) d\xi \geqslant 1. \qquad (27)$$

Considering that $\xi(x) = D(x)/D_0 - 1$, where x can be interpreted as a random variable that is uniform in the interval $[0, x_0]$, through the change-of-variables method, we can obtain $f(\xi)$. For instance, in the case of $D(x) = D_0[1 + d \cos(n\pi x/x_0)]$, considered in Sec. III B, it is $f(\xi) = [1 - \xi^2/d^2]^{-\frac{1}{2}}/(\pi d)$, for $\xi \in (-d, d)$, which substituted into Eq. (26) allows one to reobtain Eq. (25).

D. Comparison with other interpretations

In Sec. III, we presented analytical results for arbitrary $D(x)$ within the Stratonovich interpretation. Now, we will compare these results with numerical ones obtained from the integration of the stochastic differential equation (2) for other interpretations. We will use the profile $D(x) = D_0[1 + d \cos(kx)]$. Plots of the efficiency vs d are presented in Fig. 8. We consider cases where $kx_0 = n\pi$ with integer n, and hence the average level is D_0.

In Fig. 8(a), where we use profiles that are monotonic in $(0, x_0)$, we can observe several features. For $A = 1$, the efficiency is insensitive to the ordering as proved throughout this section; then there is a symmetry of inversion around $d = 0$. However, notice that this symmetry is broken for the other interpretations, meaning that the shape of the profile is relevant and not only the distribution of values when $A \neq 1$. Moreover, we observe that when the profile increases with the distance from the target ($d < 0$), the efficiency increases with larger A, while the contrary occurs for a decreasing profile ($d > 0$). Actually, this is the same behavior demonstrated analytically for the power-law case analyzed in Sec. II. Finally, note that while for $A = 1$ the efficiency remains below that of the homogeneous profile as theoretically predicted, this can
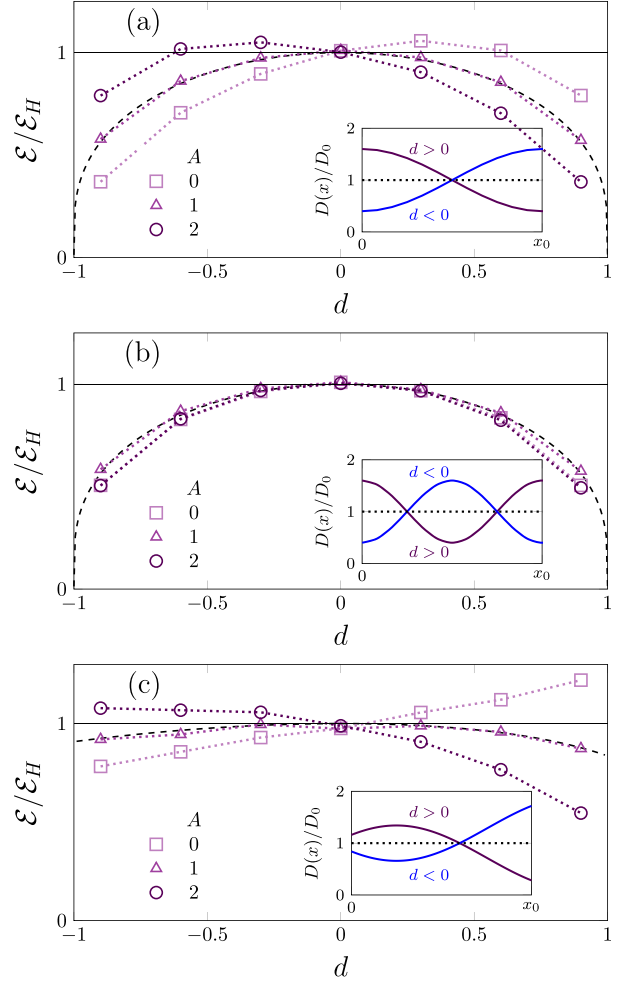

FIG. 8. Relative efficiency $\mathcal{E}/\mathcal{E}_H$ vs d, using different values of A, for the profiles (a) $D(x) = D_0[1 + d \cos(\pi x/x_0)]$, (b) $D(x) = D_0[1 + d \cos(2\pi x/x_0)]$, and (c) $D(x) = D_0[1 + d\{\cos(\pi x/x_0 - \pi/4) - A\}/(1 + A)\}]$, with $A = \sqrt{2}/\pi$. In all cases, the prediction given by Eq. (25) for the Stratonovich case (dashed line) and the homogeneous value (horizontal full line), both normalized by $\mathcal{E}_H$, is plotted. Symbols correspond to the average over 10^5 trajectories of Eq. (2), with absorbing boundary at $x = 0$. The diffusivity profiles are depicted in the insets.

be violated for the other interpretations, according to these numerical simulations.

In Fig. 8(b), where the diffusivity profiles are not monotonic but symmetric in $(0, x_0)$, the efficiency appears to also be symmetric around $d = 0$. In Fig. 8(c), with less symmetries while conserving the average in $(0, x_0)$, $\mathcal{E} > \mathcal{E}_H$ can occur when $A \neq 1$, as also observed in Fig. 8(a).

IV. FINAL REMARKS

We have derived analytical expressions for $\mathcal{E} = \langle 1/t \rangle$ as a measure of the performance of random searches when the medium is heterogeneous.

For general interpretations of the multiplicative fluctuations, characterized by parameter A, we developed the paradigmatic case with power-law diffusivity with exponent

$\alpha < 2$, which embraces the cases with increasing and decreasing mobility with the distance from the target. We observed that depending on the initial position of the searcher, there can be an optimal value of α, which depends on A. But a finite maximum does not always occur. The general feature is that for a process with larger A, the success of the search is more likely when the diffusivity increases with the distance from the target ($\alpha > 0$) and hinders the search otherwise. Moreover, this is not unique to the power-law shape, but is determined by the monotonic character of the diffusivity.

We addressed the Stratonovich framework ($A = 1$) that allows one to derive a closed expression of the efficiency for arbitrary forms of $D(x)$. In this case, we considered a localized perturbation and an oscillatory one, concluding that these heterogeneities reduce the efficiency of the homogeneous case with a level equal to the average one within $(0, x_0)$. It is important to note that the shape of the diffusivity profile within that interval is not relevant but only the set of values of the profile, which determine the integral in Eq. (21). This is a property analogous to that found in the context of critical patch size [24]. Therefore, a noisy profile with the same distribution of values yields the same results. However, beyond the Stratonovich interpretation, the shape of the profile (not only the distribution of values) may be relevant.

Note that our results can be applied to the problem of the first encounter between two walkers with trajectories $x(t)$ and $y(t)$ in one dimension, with a coupled diffusivity depending on their distance $D(|x - y|)$. For $x_0 > y_0$, $z(t) = x(t) - y(t) > 0$, and for $z(t) = 0$, the first encounter occurs. In such case, the efficiency measures the rate of success of the first encounter. This would allow one to extend previous results for the one-dimensional homogeneous case [58].

As a starting point, we addressed the HDP search problem in one dimension, but it would be interesting to extend the current results to two or three dimensions in confined systems. Consideration of colored instead of white noise is another worthwhile continuation.

ACKNOWLEDGMENTS

APPENDIX A: SOLVING EQ. (9)

First, we introduce the new function

$$\tilde{q}(x_0, s) = \tilde{Q}(x_0, s) - \frac{1}{s}, \tag{A1}$$

into Eq. (9), obtaining

$$\frac{\partial^2}{\partial x_0^2}\tilde{q}(x_0, s) + \left(1 - \frac{A}{2}\right)\frac{\alpha}{x_0}\frac{\partial}{\partial x_0}\tilde{q}(x_0, s)$$
$$- \frac{s}{D_0 x_0^\alpha}\tilde{q}(x_0, s) = 0. \tag{A2}$$

Using the change of variables

$$z = \sqrt{x_0}, \quad \tilde{q}(x_0, s) = z^\nu \tilde{w}(z, s)$$

in Eq. (A2), we get

$$\frac{\partial^2}{\partial z^2}\tilde{w}(z, s) + \frac{\mathcal{A}}{z}\frac{\partial}{\partial z}\tilde{w}(z, s)$$
$$+ \left[\frac{\mathcal{B}}{z^2} - \left(2\frac{\sqrt{s}}{\sqrt{D_0}z^{\alpha-1}}\right)^2\right]\tilde{w}(z, s) = 0, \tag{A3}$$

where $\mathcal{A} = 2\nu - 1 + (1 - A/2)2\alpha$ and $\mathcal{B} = \nu[\nu - 2 + 2\alpha(1 - A/2)]$. Equation (A3) can be identified with a Lommel-type equation [59], which admits the solution

$$\tilde{w}(z, s) = c_1 z^\beta K_b[az^{2-\alpha}] + c_2 z^\beta I_b[az^{2-\alpha}], \tag{A4}$$

where $K_b(\cdots)$ and $I_b(\cdots)$ are the modified Bessel functions [56],

$$a = \frac{2}{2-\alpha}\sqrt{\frac{s}{D_0}}, \tag{A5}$$

$$\beta = 1 - \nu - \alpha(1 - A/2), \tag{A6}$$

$$b = \pm[1 - \alpha(1 - A/2)]/(2 - \alpha), \tag{A7}$$

where the $\pm$ can be ignored since $K_b(z) = K_{-b}(z)$. To ensure the convergence of the solution $\tilde{w}(z, s)$, for large z, we must set $c_2 = 0$ into Eq. (A4). Therefore, according to Eq. (17) $\tilde{q}(x_0, s) = z^\nu w(z, s)$, we obtain

$$\tilde{q}(x_0, s) = c_1 x_0^{\frac{1}{2}(1-\alpha[1-A/2])} K_b\left(\frac{2 x_0^{\frac{2-\alpha}{2}}}{2-\alpha}\sqrt{\frac{s}{D_0}}\right). \tag{A8}$$

The probability of survival in Laplace space [see Eq. (A1)] is given by

$$\tilde{Q}(x_0, s) = c_1 x_0^{\frac{1}{2}(1-\alpha[1-A/2])} K_b\left(\frac{2 x_0^{\frac{2-\alpha}{2}}}{2-\alpha}\sqrt{\frac{s}{D_0}}\right) + \frac{1}{s},$$

where the coefficient c_1 is obtained from the boundary condition $\tilde{Q}(x_0 = x_a, s) = 0$, where x_a is the target position. Then,

$$\tilde{Q}(x_0, s) = \frac{1}{s}\left[1 - \frac{x_0^{\frac{1}{2}(1-\alpha[1-A/2])} K_b\left(\frac{2 x_0^{\frac{2-\alpha}{2}}}{2-\alpha}\sqrt{\frac{s}{D_0}}\right)}{x_a^{\frac{1}{2}(1-\alpha[1-A/2])} K_b\left(\frac{2 x_a^{\frac{2-\alpha}{2}}}{2-\alpha}\sqrt{\frac{s}{D_0}}\right)}\right],$$

and taking the limit $x_a \to 0$ in the part of function that contains the x_a parameter, we obtain

$$\mathcal{I} = \lim_{x_a \to 0} x_a^{\frac{1}{2}(1-\alpha[1-A/2])} K_b\left(\frac{2 x_a^{\frac{2-\alpha}{2}}}{2-\alpha}\sqrt{\frac{s}{D_0}}\right)$$

$$\simeq \lim_{x_a \to 0} x_a^{\frac{1}{2}(1-\alpha[1-A/2])}\frac{\Gamma[b]}{2^{1-b}}\left(\frac{2 x_a^{\frac{2-\alpha}{2}}}{2-\alpha}\sqrt{\frac{s}{D_0}}\right)^{-b}$$

$$= \lim_{x_a \to 0} x_a^{\frac{2-\alpha}{2}\left(\frac{1-\alpha[1-A/2]}{2-\alpha} - b\right)}\frac{\Gamma[b]}{2^{1-b}}\left(\frac{2}{2-\alpha}\sqrt{\frac{s}{D_0}}\right)^{-b}$$

$$= \frac{\Gamma[b]}{2^{1-b}}\left(\frac{2}{2-\alpha}\sqrt{\frac{s}{D_0}}\right)^{-b}, \tag{A9}$$

which is non-null only for $b = [1 - \alpha(1 - A/2)]/(2 - \alpha)$.

Therefore,

$$\tilde{Q}(x_0, s)$$
$$= \frac{1}{s}\left[1 - \frac{2}{\Gamma[b]}\left(\frac{x_0^{\frac{2-\alpha}{2}}}{2-\alpha}\sqrt{\frac{s}{D_0}}\right)^b K_b\left(\frac{2\,x_0^{\frac{2-\alpha}{2}}}{2-\alpha}\sqrt{\frac{s}{D_0}}\right)\right].$$
(A10)

The FPTD in Eq. (A10) is normalized only for $b > 0$; then,

$$1 - \alpha(1 - A/2) \geqslant 0. \tag{A11}$$

APPENDIX B: MEAN SQUARE DISPLACEMENT (MSD)

We calculate the second moment, which determines the asymptotic long-time limit presented in Fig. 4. To do that, we perform the average using Eq. (18) as

$$\mathcal{L}\{\langle x^2 \rangle\} = \int_0^\infty x^2 p(x, t)dx$$
$$= \int_0^\infty \frac{x^{2-\frac{\alpha}{2}}}{\sqrt{4s}}(e^{-\sqrt{s}|y(x)-y(x_0)|} - e^{-\sqrt{s}|y(x)+y(x_0)|})dx$$
$$= e^{-\sqrt{s}\,y(x_0)}\int_0^{x_0}\frac{x^{2-\frac{\alpha}{2}}}{\sqrt{4s}}e^{\sqrt{s}\,y(x)}dx$$
$$\quad + e^{\sqrt{s}\,y(x_0)}\int_{x_0}^\infty\frac{x^{2-\frac{\alpha}{2}}}{\sqrt{4s}}e^{-\sqrt{s}\,y(x)}dx$$
$$\quad - e^{-\sqrt{s}\,y(x_0)}\int_0^\infty\frac{x^{2-\frac{\alpha}{2}}}{\sqrt{4s}}e^{-\sqrt{s}\,y(x)}dx$$

$$= \frac{\sinh[\sqrt{s}\,y(x_0)]}{\sqrt{s}}\int_{x_0}^\infty x^{2-\frac{\alpha}{2}}e^{-\sqrt{s}\,y(x)}dx,$$
$$\quad + \frac{e^{-\sqrt{s}\,y(x_0)}}{\sqrt{s}}\int_0^{x_0} x^{2-\frac{\alpha}{2}}\sinh[\sqrt{s}\,y(x)]\,dx, \tag{B1}$$

where y was defined in Eq. (17). Defining $z = \sqrt{s}\,y$, we get

$$z(x) = 2s^{\frac{1}{2}}x^{1-\frac{\alpha}{2}}/(2-\alpha), \tag{B2}$$

which implies $x = c_\alpha(z/\sqrt{s})^{\frac{2}{2-\alpha}}$ with $c_\alpha = (\frac{2-\alpha}{2})^{\frac{2}{2-\alpha}}$, and

$$\mathcal{L}\{\langle x^2 \rangle\} = c_\alpha^2\frac{\sinh[\sqrt{s}\,y(x_0)]}{s^{\frac{4-\alpha}{2-\alpha}}}\int_{\sqrt{s}\,y_0}^\infty z^{\frac{4}{2-\alpha}}e^{-z}dz$$
$$\quad + c_\alpha^2\frac{e^{-\sqrt{s}\,y(x_0)}}{s^{\frac{4-\alpha}{2-\alpha}}}\int_0^{\sqrt{s}y_0} z^{\frac{4}{2-\alpha}}\sinh(z)\,dz, \tag{B3}$$

where $z(x_0) = \sqrt{s}y(x_0) \equiv \sqrt{s}y_0$.

For large t, i.e., $s \sim 0$, the first term in Eq. (B3) dominates and we obtain

$$\mathcal{L}\{\langle x^2 \rangle\}|_{s\sim 0} \simeq \frac{c_\alpha^2\,y_0}{(\sqrt{s})^{\frac{6-\alpha}{2-\alpha}}}\int_0^\infty z^{\frac{4}{2-\alpha}}e^{-z}dz$$
$$\simeq \frac{2y_0 c_\alpha^{1+\frac{\alpha}{2}}\Gamma\left[\frac{4}{2-\alpha}\right]}{(\sqrt{s})^{\frac{6-\alpha}{2-\alpha}}}. \tag{B4}$$

Therefore, we obtain the asymptotic behavior,

$$\langle x^2 \rangle \simeq \frac{2y_0 c_\alpha^{1+\frac{\alpha}{2}}\Gamma\left[\frac{4}{2-\alpha}\right]}{\Gamma\left[\frac{1}{2}\frac{6-\alpha}{2-\alpha}\right]}\,t^{\frac{2+\alpha}{2(2-\alpha)}} \sim t^{\frac{2+\alpha}{2(2-\alpha)}}. \tag{B5}$$

Notice that for $\alpha = 0$, normal diffusion is not obtained due to the presence of the absorbing wall [1].

[1] S. Redner, *A Guide to First-passage Processes* (Cambridge University Press, New York, 2001).

[2] O. Benichou, C. Loverdo, M. Moreau, and R. Voituriez, Rev. Mod. Phys. **83**, 81 (2011).

[3] V. Zaburdaev, S. Denisov, and J. Klafter, Rev. Mod. Phys. **87**, 483 (2015).

[4] L. Mirny, M. Slutsky, Z. Wunderlich, A. Tafvizi, J. Leith, and A. Kosmrlj, J. Phys. A: Math. Theor. **42**, 434013 (2009).

[5] X. Chen, X. Cheng, Y. Kang, and J. Duan, J. Stat. Mech.: Theory Expt. (2019) 033501.

[6] A. Bhattacherjee and Y. Levy, Nucleic Acids Res. **42**, 12404 (2014).

[7] W. J. O'Brien, H. I. Browman, and B. I. Evans, Am. Sci. **78**, 152 (1990).

[8] F. Bartumeus, M. G. E. da Luz, G. M. Viswanathan, and J. Catalan, Ecology **86**, 3078 (2005).

[9] G. M. Viswanathan, M. G. E. da Luz, E. P. Raposo, and H. E. Stanley, *The Physics of Foraging: An Introduction to Random Searches and Biological Encounters* (Cambridge University Press, Cambridge, 2011).

[10] R. Martínez-García, J. M. Calabrese, T. Mueller, K. A. Olson, and C. Lopez, Phys. Rev. Lett. **110**, 248106 (2013).

[11] U. Bhat and S. Redner, J. Stat. Mech.: Theory Expt. (2022) 033402.

[12] E. Castello, T. Yamamoto, F. D. Libera, W. Liu, A. F. Winfield, Y. Nakamura, and H. Ishiguro, Swarm Intell. **10**, 1 (2016).

[13] I. Pavlyukevich, J. Comput. Phys. **226**, 1830 (2007).

[14] V. V. Palyulin, V. N. Mantsevich, R. Klages, R. Metzler, and A. V. Chechkin, Eur. Phys. J. B **90**, 170 (2017).

[15] S. M. Khadem, S. H. L. Klapp, and R. Klages, Phys. Rev. Res. **3**, 023169 (2021).

[16] J. F. Rupprecht, O. Benichou, and R. Voituriez, Phys. Rev. E **94**, 012117 (2016).

[17] A. Chechkin and I. M. Sokolov, Phys. Rev. Lett. **121**, 050601 (2018).

[18] U. Bhat, C. De Bacco, and S. Redner, J. Stat. Mech.: Theory Expt. (2016) 083401.

[19] A. G. Cherstvy, A. V. Chechkin, and R. Metzler, New J. Phys. **15**, 083039 (2013).

[20] G. Pesce, A. McDaniel, S. Hottovy, J. Wehr, and G. Volpe, Nat. Commun. **4**, 2733 (2013).

[21] N. Leibovich and E. Barkai, Phys. Rev. E **99**, 042138 (2019).

[22] S. Pieprzyk, D. Heyes, and A. Brańka, Biomicrofluidics **10**, 054118 (2016).

[23] A. Berezhkovskii and D. Makarov, J. Chem. Phys. **147**, 201102 (2017).

[24] M. A. F. dos Santos, V. Dornelas, E. H. Colombo, and C. Anteneodo, Phys. Rev. E **102**, 042139 (2020).

[25] M. A. F. dos Santos, E. H. Colombo, and C. Anteneodo, Chaos Solitons Fractals **152**, 111422 (2021).

[26] B. Oksendal, *Stochastic Differential Equations: An Introduction with Applications* (Springer Science & Business Media, New York, 2013).

[27] H. Risken, *The Fokker-Planck Equation*, 2nd ed. (Springer-Verlag, Berlin, 1989).

[28] G. Vaccario, C. Antoine, and J. Talbot, Phys. Rev. Lett. **115**, 240601 (2015).

[29] K. Itô, Proc. Imp. Acad. **20**, 519 (1944).

[30] R. L. Stratonovich, SIAM J. Control **4**, 362 (1966).

[31] P. Hanggi, Phys. Rev. A **25**, 1130 (1982).

[32] Y. L. Klimontovich, Phys. A: Stat. Mech. Appl. **163**, 515 (1990).

[33] G. Volpe, L. Helden, T. Brettschneider, J. Wehr, and C. Bechinger, Phys. Rev. Lett. **104**, 170602 (2010).

[34] T. Brettschneider, G. Volpe, L. Helden, J. Wehr, and C. Bechinger, Phys. Rev. E **83**, 041113 (2011).

[35] S. Hottovy, G. Volpe, and J. Wehr, J. Stat. Phys. **146**, 762 (2012).

[36] M. A. F. dos Santos and I. S. Gomez, J. Stat. Mech.: Theory Expt. (2018) 123205.

[37] P. C. Bressloff and S. D. Lawley, Phys. Rev. E **95**, 060101(R) (2017).

[38] A. Godec and R. Metzler, Phys. Rev. E **91**, 052134 (2015).

[39] N. M. Mutothya, Y. Xu, Y. Li, R. Metzler, and N. M. Mutua, J. Phys. Complex. **2**, 045012 (2021).

[40] S. Ray, J. Chem. Phys. **153**, 234904 (2020).

[41] T. Sandev, V. Domazetoski, L. Kocarev, R. Metzler, and A. Chechkin, J. Phys. A: Math. Theor. **55**, 074003 (2022).

[42] T. Sandev, A. Iomin, and L. Kocarev, Phys. Rev. E **102**, 042109 (2020).

[43] A. James, J. W. Pitchford, and M. J. Plank, Bull. Math. Biol. **72**, 896 (2010).

[44] V. V. Palyulin, A. V. Chechkin, and R. Metzler, Proc. Natl. Acad. Sci. USA **111**, 2931 (2014).

[45] V. V. Palyulin, A. V. Chechkin, and R. Metzler, J. Stat. Mech.: Theory Expt. (2014) P11031.

[46] T. Sandev, A. Iomin, and L. Kocarev, J. Phys. A: Math. Theor. **52**, 465001 (2019).

[47] A. Padash, T. Sandev, H. Kantz, R. Metzler, and A. V. Chechkin, Fractal Fract. **6**, 260 (2022).

[48] V. V. Palyulin, A. V. Chechkin, R. Klages, and R. Metzler, J. Phys. A: Math. Theor. **49**, 394002 (2016).

[49] T. Sandev, A. Schulz, H. Kantz, and A. Iomin, Chaos, Solitons Fractals **114**, 551 (2018).

[50] B. O'Shaughnessy and I. Procaccia, Phys. Rev. Lett. **54**, 455 (1985).

[51] P. Singh, Phys. Rev. E **105**, 024113 (2022).

[52] A. Celani, E. Villermaux, and M. Vergassola, Phys. Rev. X **4**, 041015 (2014).

[53] M. Durve, L. Piro, M. Cencini, L. Biferale, and A. Celani, Phys. Rev. E **102**, 012402 (2020).

[54] H. Sanhedrai and Y. Maayan, Phys. Rev. E **103**, 012114 (2021).

[55] M. Naguib and R. H. Wiley, Anim. Behav. **62**, 825 (2001).

[56] M. Abramowitz and I. A. Stegun, *Handbook of Mathematical Functions with Formulas, Graphs, and Mathematical Tables* (Dover Publications Inc., Mineola, NY, 1964).

[57] L. Angelani and R. Garra, Phys. Rev. E **100**, 052147 (2019).

[58] F. Le Vot, S. B. Yuste, E. Abad, and D. S. Grebenkov, Phys. Rev. E **102**, 032118 (2020).

[59] D. Zwillinger and A. Jeffrey, *Table of Integrals, Series, and Products* (Elsevier, Amsterdam, 2007).